Supporting information

1. Self-assembly of AgNC

SEM images in Figure S1 show the AgNCs' distribution on silicon surface, which depends on the AgNC's concentration and deposition conditions. A high concentration of AgNC (without dilution) leaded to the stacks of AgNCs on the surface (not shown here) so that a spinning coating (at ~800 rpm) has been employed for deposition. In Figures S1 (a) and (b), there are crystalline areas with high density of juxtaposed facets along domain's edge at its peripheral (a) and central parts (b), which is likely due to the capillary force along the domain edge to push AgNCs into a dense arrangement by self-assembly.[1] However, this arrangement is uncontrollable and shows a high density of defect (top-right area in Figure S1 (a)). Moreover, the main components along the edge are not NCs but nanoparticles (bottom-left area in Figure S1 (a)) due to the extraction occurring within a domain with large scale (> 1μm^2). We thus selected PSNS to template the surface and to shrink the domain's size.

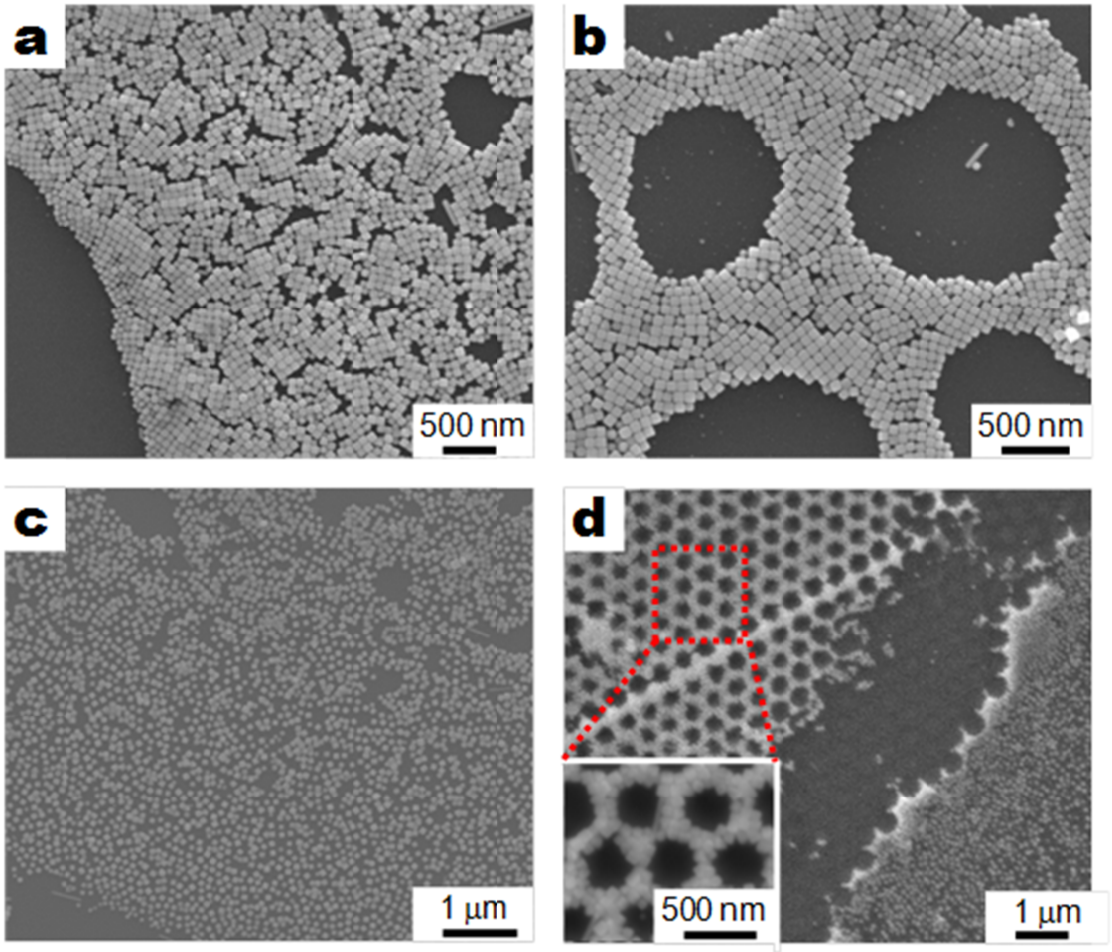

Figure S1: SEM images showing the arrangement of AgNCs. On blank surface without PSNS template (a–c), high concentration of AgNC (without dilution) features crystalline areas along the domain's edge at the peripheral (a) and central parts (b). Low concentration (diluted to 1:2, v/v) features a random distribution (c). When PSNS template has been used, an ordered and dense arrangement of AgNC is obtained in (d) (top-left area and inset) whilst the random distribution is still observed in the bottom-right area when the PSNS template is absent.

However, high concentration of AgNC featured stacks of AgNCs in the presence of PSNS template, as shown in Figures 2 (e–f). We therefore diluted the AgNC solution to 1:2 (v/v) using methanol containing a small amount of Triton-x-100. Figure S1 (c) shows that without the PSNS template, AgNCs distribute randomly on the surface. In the presence of PSNS template, we observed the ordered and densely-arranged AgNC array in Figure S1 (d) (top-left area and inset). When the PSNS template is absent, a random distribution is obtained in the right-bottom area. We thus assigned the main driving force for self-assembly of AgNC to the capillary force during the drying process of the AgNC aqueous solution underneath the PSNS template. [1]

2. Raman comparison

We characterized the Raman enhancement of the AgNC arrays. Figure S2 (a) shows the optical image, in which the AgNC array templated by PSNS is visible on the top. On the bottom (left and right), there is no template. Their typical SEM images are presented in Figures S2 (b) and (c), which are collected from the marked areas in (a).

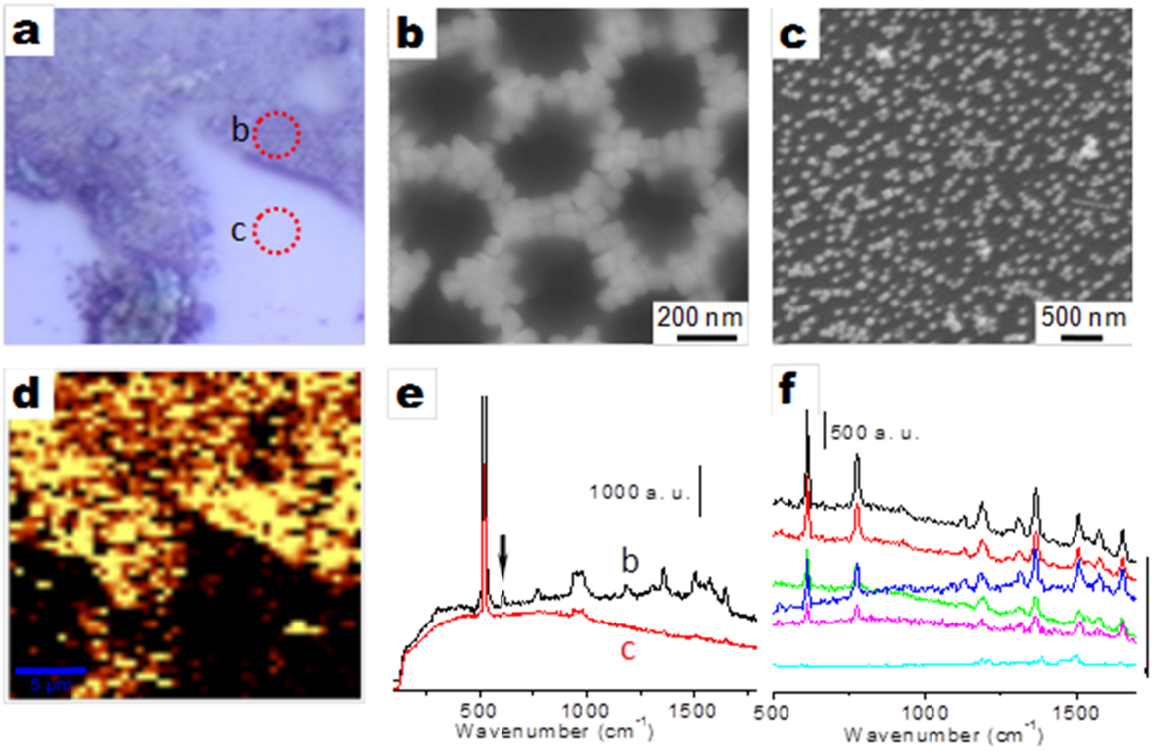

Figure S2: Raman and SEM characterization of AgNC arrays. (a) shows the optical image of the surface whilst (b) and (c) the typical SEM images from the marked areas. (d) shows the Raman mapping image of (a) based on R6G peak at ~613 cm^{-1} (indicated in (e)). (e, f) show the typical Raman spectra of R6G. The spectra in (e) were collected from the marked areas in (a). In (f), from top to bottom, the corresponding surface morphology is presented in Figure 2 (c), Figure 2 (b), Figure 2 (a), Figure 2 (d), Figure 2 (f), Figure S1 (c), respectively. For R6G loading, a drop of (~10 μl) 1×10^{-6} M R6G was spread on the surface and dried in air. The silicon peaks were removed by subtracting the silicon's Raman spectrum. The scale bar in (a) is the same as that in (d).

Figure S2 (d) shows the Raman mapping result based on R6G's intensity of the characteristic peak at ~613 cm^{-1}, which is indicated with an arrow in Figure S2 (e) where the typical Raman spectra collected from the marked area in (a) are shown. The templated AgNC array area feature higher intensity (100-200 times) of Raman signal than the no-template area does, suggesting the enhancement originating from the ordered AgNC area. [1a, 2] This result is in well agreement with that shown in Figure 3 where silicon's Raman signal has been enhanced from the ordered AgNC area due to existence of the juxtaposed facets.

We also tested the enhancement of the different morphology of AgNC array using R6G as a Raman probe. Figure S2 (e) shows the typical spectra of R6G collected from the different surface, the topographies of which are presented in Figure 2 (c), Figure 2 (b), Figure 2 (a), Figure 2 (d), Figure 2 (f), Figure S1 (c), respectively from top to bottom. The structure presented in Figure 2 (c) (also in Figure S1 (d)(inset), Figure S2 (b)) emit the strongest Raman signal so that its deposition condition (1:2 dilution, v/v) has been selected for the following experiments.

3. Loading MPy onto AgNC

We immersed the DDT_AgNC in a MPy solution (1×10^{-5} M) for 72 h (rather than 1 h, the shortest time needed to observe the MPy's Raman scattering). We found the corners of most AgNCs have been polished from a square one into a round one, as shown in Figures S3 (a) (before loading) and (b) (after loading). The typical morphology of individual AgNC is shown in the insets, suggesting the loading of MPy indeed take place at the pinhole of DDT SAM, which is localized at the AgNC's corner. [3] In (b), the geometry-shape of a cube, not a sphere, is still observable, suggesting the main loading position of MPy is at the corners rather than along the edges.

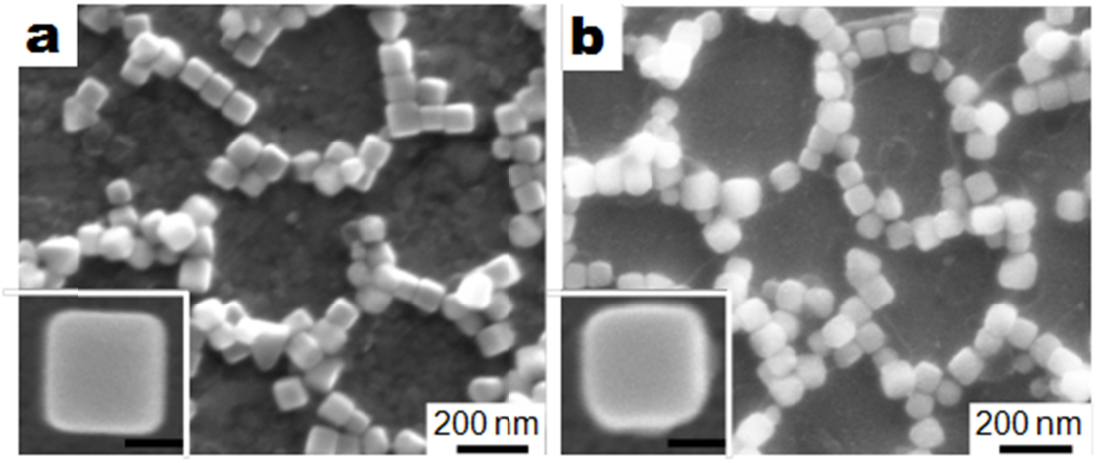

Figure S3: SEM images before (a) and after (b) <MPy loading. AgNC array (corresponding to Figure 4 (e)) was incubated in an ethanol solution containing DDT (0.1 %, v/v) for 2 h for DDT SAM to be formed (a). The DDT_AgNC array was further incubated in an aqueous solution containing MPy (1×10^{-5} M) for 72 h (b). Insets show the typical morphology of the individual AgNC with scale bar of 25 nm.

4. Self-assembly of AuNP

Figure S4 shows the PSNS mask can also template AuNPs from diameter of ~50 nm to ~125 nm. The deposition of AuNP was carried out under the similar conditions with that of AgNC, suggesting a universal approach to template the nano components.

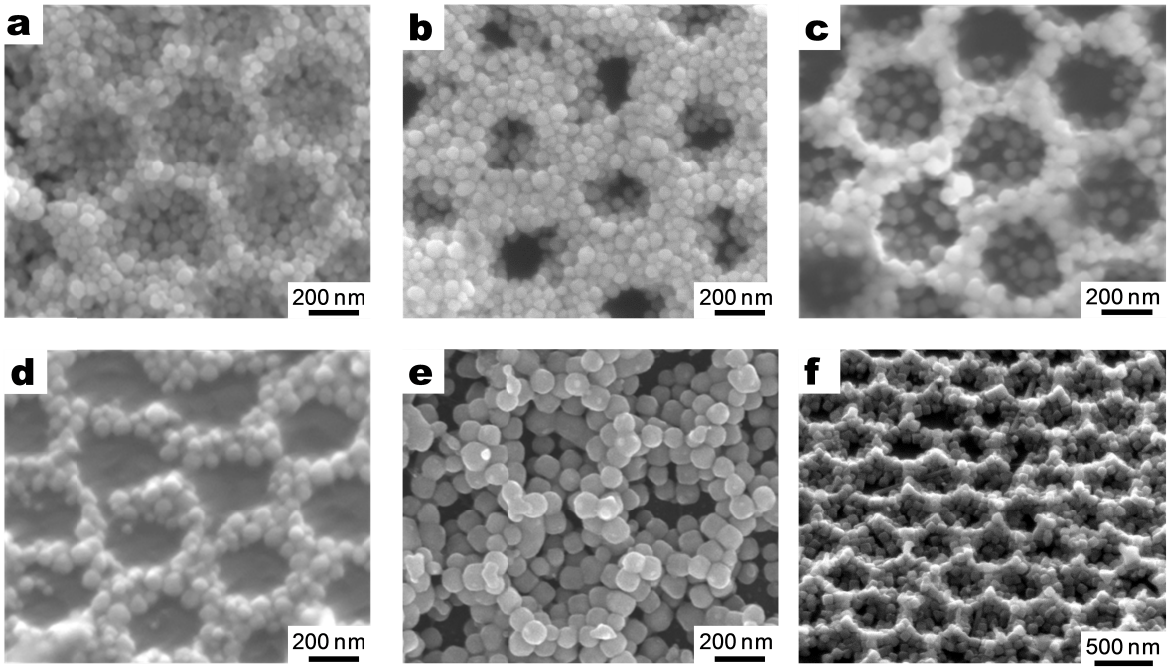

Figure S4: Templated AuNPs with diameter of 50 nm (a, b), 75 nm (c, d) and 125 nm (e, f). The deposition protocol is similar with that for AgNC deposition.

References

[1] a)M. Rycenga, C. M. Cobley, J. Zeng, W. Li, C. H. Moran, Q. Zhang, D. Qin, Y. Xia, *Chemical Reviews* **2011**, *111*, 3669; b)M. R. Jones, K. D. Osberg, R. J. Macfarlane, M. R. Langille, C. A. Mirkin, *Chemical Reviews* **2011**, *111*, 3736.

[2] a)S. Y. Lee, L. Hung, G. S. Lang, J. E. Cornett, I. D. Mayergoyz, O. Rabin, *ACS Nano* **2010**, *4*, 5763; b)S. Mazzucco, N. Geuquet, J. Ye, O. Stéphan, W. Van Roy, P. Van Dorpe, L. Henrard, M. Kociak, *Nano Letters* **2012**.

[3] a)A. Ulman, *Chemical Reviews* **1996**, *96*, 1533; b)K. Edinger, A. Goelzhaeuser, K. Demota, C. Woell, M. Grunze, *Langmuir* **1993**, *9*, 4; c)S. J. Stranick, A. N. Parikh, Y. T. Tao, D. L. Allara, P. S. Weiss, *The Journal of Physical Chemistry* **1994**, *98*, 7636; d)D. K. Schwartz, *Annual Review of Physical Chemistry* **2001**, *52*, 107.